Kernels and integration cycles in complex Langevin simulations

Michael Mandl,[a,*] **Michael W. Hansen,**[a] **Erhard Seiler**[b] **and Dénes Sexty**[a]

[a]*Institute of Physics, NAWI Graz, University of Graz,*
Universitätsplatz 5, 8010 Graz, Austria

[b]*Max-Planck-Institut für Physik (Werner-Heisenberg-Institut),*
Boltzmannstraße 8, 85748 Garching bei München, Germany
E-mail: michael.mandl@uni-graz.at, michael.hansen@uni-graz.at,
ehs@mpp.mpg.de, denes.sexty@uni-graz.at

The method of complex Langevin simulations is a tool that can be used to tackle the complex-action problem encountered, for instance, in finite-density lattice quantum chromodynamics or real-time lattice field theories. The method is based on a stochastic evolution of the dynamical degrees of freedom via (complex) Langevin equations, which, however, sometimes converge to the wrong equilibrium distributions. While the convergence properties of the evolution can to some extent be assessed by studying so-called boundary terms, we demonstrate in this contribution that boundary terms on their own are not sufficient as a correctness criterion. Indeed, in their absence complex Langevin simulation results might still be spoiled by unwanted so-called integration cycles. In particular, we elaborate on how the introduction of a kernel into the complex Langevin equation can – in principle – be used to control which integration cycles are sampled in a simulation such that correct convergence is restored.

---

*Speaker

1. Introduction

The study of quantum chromodynamics (QCD) at non-zero chemical potential is notoriously difficult due to the infamous sign or complex-action problem preventing the use of straightforward lattice quantum field theory methods based on importance sampling. Nonetheless, a proper understanding of the finite-density region of the QCD phase diagram is of fundamental importance for the correct description of, e.g., neutron stars or the heavy-ion collision experiments at RHIC or the LHC. One particular method that has seen progress in recent years in the context of finite-density QCD [1–4] as well as various other theories plagued by a sign problem, such as the real-time evolution of lattice field theories [5, 6], is the complex Langevin method, which is based on a complexified version of the well-known Langevin equation [7, 8]. It avoids the sign problem by trading the complex weight e^{-S} in the conventional Euclidean path integral for a genuine probability density in complexified field space. However, the complex Langevin approach does not come without its own set of problems, as it, for instance, sometimes produces wrong results despite apparently properly converging to equilibrium. Thus, an important milestone in the development of the complex Langevin method would be to establish a sensible criterion of correctness that could detect such incorrect convergence. One candidate for a correctness criterion of this kind is the study of boundary terms, the appearance of which spoils the formal proof of convergence of the method [9, 10]. As we demonstrate in this contribution, however, this criterion is not always reliable as it may sometimes falsely indicate correct results. The origin of this failure is contributions from unwanted so-called integration cycles. In this contribution, we show how to – in principle – remove these contributions via the introduction of a kernel into the complex Langevin equation.

2. Complex Langevin equation and boundary terms

The (complex) Langevin equation is a stochastic differential equation describing the evolution of a physical system in an auxiliary time direction τ, the so-called Langevin time. For a single (complex) degree of freedom $z = x + \mathrm{i}y$, it reads

$$\frac{dz(\tau)}{d\tau} = -K\frac{\partial S(z)}{\partial z} + \sqrt{K}\eta(\tau) \,, \tag{1}$$

where S denotes the action of the theory, $S(x)$, analytically continued to complex arguments and η is real Gaussian random noise with the properties $\langle\eta(\tau)\rangle = 0$ and $\langle\eta(\tau)\eta(\tau')\rangle = 2\delta(\tau - \tau')$. Moreover, K denotes the so-called kernel that can be used to control the convergence properties of the evolution. It is chosen constant, i.e., independent of z, here for simplicity albeit this choice could easily be relaxed.

The stochastic evolution (1) gives rise to a probability density $P(x, y; \tau)$ in the complex plane and the complex Langevin approach solves the sign problem if and only if this probability density is equivalent to the target complex weight e^{-S} of the original ("path") integral, $Z = \int dx e^{-S(x)}$, in the sense that

$$\lim_{\tau\to\infty}\int dxdy P(x, y; \tau)O(x + \mathrm{i}y) = \frac{1}{Z}\int dx e^{-S(x)}O(x) \tag{2}$$

for all holomorphic observables O. In the case of a real action S, a similar convergence condition can indeed be proven under very mild assumptions [11]. For complex S, on the other hand, a sound

2

mathematical formulation does not exist and, in fact, the complex Langevin equation in some cases fails to produce correct results entirely, as we shall demonstrate in the remainder of this work.

Part of this failure can be traced back to an insufficient decay of $P(x, y; \tau)$ in the complex plane, which spoils the formal proof of correctness of the complex Langevin approach (relying on integration by parts) due to the appearance of boundary terms at infinity [9, 10]. It is possible in principle to measure these boundary terms in a simulation [12] via the observable

$$\mathcal{B}_{O(z)}(Y) = \langle \Theta\left(Y - |z|\right) LO(z) \rangle \; , \tag{3}$$

where $L = \left(\frac{\partial}{\partial z} - \frac{\partial S(z)}{\partial z}\right) K \frac{\partial}{\partial z}$ and Y denotes a cutoff one imposes on the distribution in the complex plane in order to alleviate signal-to-noise problems. In practice, one looks for a plateau in $\mathcal{B}_{O(z)}(Y)$ and extrapolates to $Y \to \infty$. Indeed, if such a plateau is assumed at a non-vanishing value of $\mathcal{B}_{O(z)}$, one concludes that correct convergence cannot be proven as the integration by parts cannot be performed and, thus, that the obtained simulation results must be incorrect. The converse, however, is not necessarily true. Indeed, as has been shown in [13] and as we shall substantiate in this contribution, the absence of boundary terms does not automatically imply the correct convergence of a complex Langevin simulation. The reason for this is outlined in the subsequent section.

3. Integration cycles

It was shown in [13] that vanishing boundary terms do not guarantee the convergence of results obtained in a complex Langevin simulation, $\langle O \rangle_{\text{CL}}$, to the correct values $\langle O \rangle_{\text{exact}}$, but rather, as was surmised already in [14], that the former are given by a linear combination of observables computed along so-called integration cycles γ_i,

$$\langle O \rangle_{\text{CL}} = \sum_{i=1}^{N_\gamma} a_i \langle O \rangle_{\gamma_i} \; , \quad \sum_{i=1}^{N_\gamma} a_i = 1 \; , \tag{4}$$

where the a_i are complex coefficients independent of the observables and we have defined

$$\langle O \rangle_{\gamma_i} := \frac{\int_{\gamma_i} dz e^{-S(z)} O(z)}{\int_{\gamma_i} dz e^{-S(z)}} \; . \tag{5}$$

The cycles γ_i are defined to be integration paths in the complex plane that either connect two distinct zeros of the weight e^{-S} (including those at complex infinity) or are closed incontractible loops, while N_γ denotes the number of such integration cycles that are linearly independent of one another. If one defines γ_1 such that $\langle O \rangle_{\gamma_1} = \langle O \rangle_{\text{exact}}$, the complex Langevin evolution produces correct results if and only if $a_i = \delta_{i,1}$. Since – in general – neither the a_i nor the $\langle O \rangle_{\gamma_i}$ are known *a priori*, a natural question that arises is whether one has any sort of control over the coefficients in practice in order to meet this condition.

It was found in [15] that the equilibrium solutions produced by the complex Langevin equation can be influenced by the choice of kernel K in (1), an observation that was further elaborated on in [14]. Indeed, as we show below, the coefficients a_i in (4) depend on K in some way. To see how, we follow [15] by considering the following simple toy model:

$$S = \frac{\lambda_l}{4} z^4 \; , \quad \lambda_l := e^{\mathrm{i}\pi l/6} \; , \quad l \in \{-5, \dots, 6\} \; . \tag{6}$$

Table 1: Expectation value $\langle z^2 \rangle$ in the model (6) for different values of l (first column), both computed exactly via (7) (second column) and in a complex Langevin simulation (third column). We also show the boundary term $\mathcal{B}_{z_2}$ for $\langle z^2 \rangle$ evaluated at some representative value Y_{plat} where $\mathcal{B}_{z^2}(Y)$ forms a plateau (last column). The numerical results are rounded to the first significant digit of their estimated jackknife error.

l	$\langle z^2 \rangle_{\text{exact}}$	$\langle z^2 \rangle_{\text{CL}}$	$\mathcal{B}_{z^2}(Y_{\text{plat}})$
-5	$0.174956 + 0.652945\,\mathrm{i}$	$-0.652933(8) + 0.17497(2)\,\mathrm{i}$	$0.0000(2) - 0.0002(3)\,\mathrm{i}$
-4	$0.337989 + 0.585414\,\mathrm{i}$	$-0.40380(2) + 0.44282(2)\,\mathrm{i}$	$1.37(2) - 2.37(2)\,\mathrm{i}$
-3	$0.477989 + 0.477989\,\mathrm{i}$	$0.41415(2) + 0.50696(1)\,\mathrm{i}$	$0.001(2) - 0.326(2)\,\mathrm{i}$
-2	$0.585414 + 0.337989\,\mathrm{i}$	$0.58543(1) + 0.33801(1)\,\mathrm{i}$	$-0.00013(6) - 0.00006(2)\,\mathrm{i}$
-1	$0.652945 + 0.174956\,\mathrm{i}$	$0.65294(1) + 0.174953(5)\,\mathrm{i}$	$0.00002(6) + 0.00001(1)\,\mathrm{i}$
0	$0.675978 + 0.000000\,\mathrm{i}$	$0.67598(2) + 0.00000\,\mathrm{i}$	$0.00002(5) + 0.00000\,\mathrm{i}$
1	$0.652945 - 0.174956\,\mathrm{i}$	$0.65296(2) - 0.174962(8)\,\mathrm{i}$	$-0.00008(6) + 0.00001(1)\,\mathrm{i}$
2	$0.585414 - 0.337989\,\mathrm{i}$	$0.58542(1) - 0.33801(1)\,\mathrm{i}$	$-0.00010(6) + 0.00008(3)\,\mathrm{i}$
3	$0.477989 - 0.477989\,\mathrm{i}$	$0.41414(2) - 0.50696(1)\,\mathrm{i}$	$-0.001(1) + 0.328(1)\,\mathrm{i}$
4	$0.337989 - 0.585414\,\mathrm{i}$	$-0.40392(4) - 0.44275(9)\,\mathrm{i}$	$1.370(5) + 2.377(5)\,\mathrm{i}$
5	$0.174956 - 0.652945\,\mathrm{i}$	$-0.652953(9) - 0.17495(2)\,\mathrm{i}$	$0.0003(1) + 0.0001(1)\,\mathrm{i}$
6	$0.000000 + 0.675978\,\mathrm{i}$	$-0.675981(6) - 0.00003(3)\,\mathrm{i}$	$0.00006(5) + 0.00006(7)\,\mathrm{i}$

It was shown in [15] that with a trivial kernel, $K = 1$, the complex Langevin evolution converges to the analytical solution for the expectation value of the observable $O(z) = z^2$,

$$\langle z^2 \rangle_{\text{exact}} = \left(\frac{4}{\lambda_l} \right)^{1/2} \frac{\Gamma(3/4)}{\Gamma(1/4)} \, , \tag{7}$$

to a satisfactory degree as long as $-2 \lesssim l \lesssim 2$ but fails outside that interval. We have reproduced these results using an improved discretization of the Langevin equation including an adaptive step-size algorithm (the precise technical details will be published elsewhere) and we summarize our findings, including the corresponding boundary terms $\mathcal{B}_{z^2}$ from (3), in Table 1.

The curious point to note is the following: While the study of boundary terms can detect the success or failure of a simulation correctly for most values of λ_l, it fails for $l = -5$, 5 and 6. For these values, the boundary terms are very small and most likely consistent with zero within discrete-step-size and round-off errors even though the stochastic evolution converges to an equilibrium distribution that gives incorrect results for holomorphic observables. This observation shows that the study of boundary terms is not sufficient in certain cases. Recall, however, that up to now we have only considered a single observable, $\langle z^2 \rangle$, and the boundary term associated with it.

Let us now discuss the role of the kernel in (1). By parametrizing it as

$$K = K_m := e^{-\mathrm{i}\pi m/24} \, , \quad m \in \{0, \ldots, 47\} \, , \tag{8}$$

we may study the dependence of observables on m. Considering $l = 5$ in (6), we show the dependence of $\langle z^2 \rangle$ on m in Fig. 1 (left). Indeed, as was also shown in [15], there is a plateau around $m = 10$ on which the analytical result (7) is reproduced.[1] Moreover, we find that on this plateau the

---

[1]We mention in passing that close to $m = 10$ the kernel has the effect of aligning the distribution of z in the complex plane with the relevant Lefschetz thimble. For a discussion on the role of Lefschetz thimbles in the context of complex Langevin simulations, see, e.g., [16].
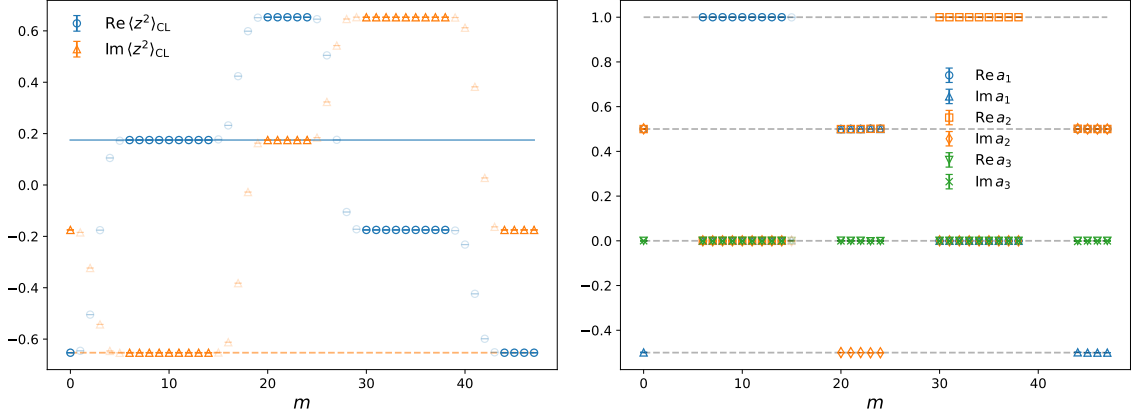
Figure 1: *Left:* Expectation value $\langle z^2 \rangle$ in the model (6) for $l = 5$ as a function of m in (8). We also show the real and imaginary parts of the exact result (7) as solid and dashed horizontal lines, respectively. *Right:* Coefficients a_i for the same setup, computed from (4) using $\langle z \rangle_{\mathrm{CL}}$, $\langle z^2 \rangle_{\mathrm{CL}}$, and $\langle z^4 \rangle_{\mathrm{CL}}$. We only show data points for which the coefficients could be determined consistently. The dashed horizontal lines mark the values $-0.5, 0, 0.5$, and 1 for convenience. In both figures, the data points for which the boundary terms are not clearly nonzero are highlighted.

boundary terms $\mathcal{B}_{z^2}$ are consistent with zero. Notice, however, that there are additional plateaus, around $m = 22, 34$, and 46, respectively, on which boundary terms vanish but the complex Langevin result nonetheless disagrees with the exact one. From the theorem (4), we thus conclude that close to $m = 10$ one must have $a_i = \delta_{i,1}$, as desired, whereas outside this region other integration cycles also contribute non-negligibly. Let us now quantify this statement.

To this end, we first count the number of independent integration cycles N_γ of the theory (6), setting $\lambda_l = 1$ for now without loss of generality. It is not hard to see that e^{-S} vanishes in four disconnected regions around $z = \pm\infty$ and $z = \pm i\infty$, respectively. This leaves us (up to homology) with six possible integration cycles in total, only $N_\gamma = 3$ of which are linearly independent, as can be shown using basic sum rules of line integrals. We may, for instance, choose the following basis set of integration cycles:

$$\int_{\gamma_1} dz := \int_{-\infty}^{\infty} dz \,, \quad \int_{\gamma_2} dz := \int_{-i\infty}^{i\infty} dz \,, \quad \int_{\gamma_3} dz := \int_{i\infty}^{\infty} dz \,. \tag{9}$$

We emphasize that the precise shape of the integration contours in (9) is irrelevant due to Cauchy's theorem as we only consider holomorphic observables; the cycles are thus uniquely specified by their respective end points.

For general λ_l in the model (6), we define γ_1 to be the real line rotated by an angle $\theta = \arg(\sqrt[4]{\lambda^{-1}})$. On such an integration contour S is real and positive. The other cycles γ_2 and γ_3 are then defined analogously via a rotation of the paths given in (9). The expectation values $\langle z^n \rangle_{\gamma_i}$, defined in (5), can be computed exactly for all such γ_i and positive integers n. This allows one to extract the coefficients a_i from (4) by measuring a sufficiently large set of monomial observables $\langle z^n \rangle_{\mathrm{CL}}$. Since $\sum_{i=1}^{N_\gamma} a_i = 1$ eliminates one (complex) degree of freedom, one requires a minimum of $N_\gamma - 1 = 2$ observables for the fit. Note, however, that $\langle z^{4n+3} \rangle_{\gamma_i} = 0$ for all i, which excludes the use of such powers. Here, we determine the coefficients by measuring $\langle z \rangle_{\mathrm{CL}}$, $\langle z^2 \rangle_{\mathrm{CL}}$, and $\langle z^4 \rangle_{\mathrm{CL}}$ in order to

ensure that the fit is stable, while at the same time avoiding the large fluctuations encountered for higher powers. Doing so for different values of m at $l = 5$, we obtain the dependence of a_i on the kernel shown in Fig. 1 (right). As expected, we find that around $m = 10$ all coefficients except $a_1 = 1$ vanish. On the contrary, close to $m = 34$ it is the second cycle that dominates. For other values of m with vanishing boundary terms, one finds different linear combinations of the $\langle O \rangle_{\gamma_i}$ to contribute, all in accordance with (4). Notice that even for certain kernels where there are non-zero boundary terms, in which case (4) has not been proven to apply, we nonetheless obtain more or less reasonable fits. It is also striking to observe that a_3 is consistent with zero for all values of m shown. This fact is noteworthy since it occurs only when averaging over multiple independent simulation runs. On the contrary, for appropriate subsets of runs with similar initial configurations, we observe non-ergodicity in certain cases, which may then give rise to non-vanishing values of a_3. We shall discuss this issue in more detail in a forthcoming publication.

These observations make clear that a kernel K in (1) can have a non-trivial influence on the integration cycles that are sampled in a complex Langevin simulation. In the simple example considered here, it is not hard to understand why a kernel of the form (8) with $m \approx 10$ gives rise to correct results in the theory (6) with $l = 5$. After all, with this choice the complex Langevin dynamics (1) becomes equivalent to real Langevin dynamics (albeit on a rotated "real" axis as defined above) [15], which can be shown to converge. In more realistic theories, however, one can only guess what an appropriate kernel could be. Hence, a better understanding of how (if at all) kernels can influence the convergence, as well as which integration cycles are sampled in a simulation, would be very much desirable. Obviously, in more complicated theories one cannot simply compute the $\langle O \rangle_{\gamma_i}$ and then fit the coefficients a_i, as the former would already amount to solving the theory altogether. In fact, in general it is very difficult to determine what the independent cycles γ_i are in the first place. Moreover, the theorem (4) was only proven for a single degree of freedom to begin with. As a first step towards a better understanding of the role of integration cycles in realistic theories, we thus devote the remainder of this work to a numerical study of the validity of (4) for two degrees of freedom.

4. Integration cycles in two dimensions

Let us consider the following straightforward extension of the model (6) to two degrees of freedom, z_1 and z_2:

$$S = \frac{\lambda_l}{4}(z_1^2 + z_2^2)^2 \, , \tag{10}$$

where we once more parametrize λ_l as in (6). The concept of integration cycles is generalized to d dimensions rather straightforwardly as d-dimensional integration paths in $\mathbb{C}^d$ that either connect two distinct zeros of e^{-S} or are closed and incontractible. As before, in the model (10) we do not need to worry about the latter, nor about finite zeros, as e^{-S} has no singularities and only vanishes as $|z_i| \to \infty$. In particular, there are zeros whenever $\mathrm{Re}\, S \to \infty$ as $|z_i| \to \infty$. To find the independent integration cycles of (10), we shall first determine these zeros.

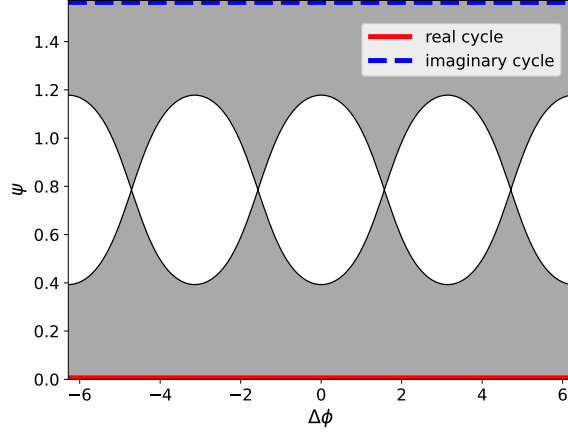Introducing the real and imaginary parts of z_i as $z_i = x_i + iy_i$, we choose the following –

Figure 2: Sign of $P(\phi_x, \phi_y, \psi)$ in (12) in the $(\Delta\phi, \psi)$ plane. In the shaded regions $P(\phi_x, \phi_y, \psi) > 0$, such that e^{-S} vanishes in the limit $r \to \infty$, while in the white regions $P(\phi_x, \phi_y, \psi) \leq 0$. The real and imaginary integration cycles in these coordinates are marked as full and dashed lines, respectively.

convenient, but perhaps unusual – parametrization:

$$
\begin{aligned}
x_1 &= r_x \cos(\phi_x) , & x_2 &= r_x \sin(\phi_x) , & r_x &= r \cos(\psi) , \\
y_1 &= r_y \cos(\phi_y) , & y_2 &= r_y \sin(\phi_y) , & r_y &= r \sin(\psi) ,
\end{aligned}
\tag{11}
$$

such that $\psi = \arctan\left(\frac{r_y}{r_x}\right) \in \left[0, \frac{\pi}{2}\right]$. Inserting (11) back into (10), we obtain the following expression for the real part of S, again assuming $\lambda_l = 1$ without loss of generality:

$$
\operatorname{Re} S = r^4 P(\phi_x, \phi_y, \psi) , \quad P(\phi_x, \phi_y, \psi) = \cos^2(2\psi) - \sin^2(2\psi) \cos^2(\phi_x - \phi_y) .
\tag{12}
$$

Notice how the latter expression depends only on the difference $\Delta\phi := \phi_x - \phi_y$, which nicely reflects the O(2) symmetry of (10). We have thus reduced the problem of finding the zeros of e^{-S} to the problem of finding regions in $(\Delta\phi, \psi)$ space where $P(\phi_x, \phi_y, \psi) > 0$. We show a plot of the sign of $P(\phi_x, \phi_y, \psi)$ in Fig. 2.

The integration cycles can now be understood as incontractible paths within the $P > 0$ regions, of which, as one can see from Fig. 2, there are only two. Taking into account the periodicity in $\Delta\phi$, this suggests that there exist (up to homology) $N_\gamma = 2$ independent integration cycles, one for $\psi \lessgtr \frac{\pi}{4}$, respectively, and we have indicated these cycles in Fig. 2. Upon closer inspection, it turns out that the cycle in the region $\psi < \frac{\pi}{4}$ is equivalent to the real integration cycle γ_1, while the one for $\psi > \frac{\pi}{4}$ corresponds to the imaginary cycle γ_2. Here, we have defined (still assuming $\lambda_l = 1$)

$$
\iint_{\gamma_1} dz_1 dz_2 := \int_{-\infty}^{\infty} dz_1 \int_{-\infty}^{\infty} dz_2 , \quad \iint_{\gamma_2} dz_1 dz_2 := \int_{-i\infty}^{i\infty} dz_1 \int_{-i\infty}^{i\infty} dz_2 .
\tag{13}
$$

For general λ_l, the γ_i are once again defined via appropriate rotations of the real and imaginary lines, as above. It is curious to note that the number of independent integration cycles in the model (10) is, in fact, smaller than in its one-dimensional counterpart (6). This observation, however, is due to the particular definition of S in (10). For instance, the model $S = z_1^4 + z_2^4$, which trivially decomposes into two independent one-dimensional models of the type (6), features nine instead
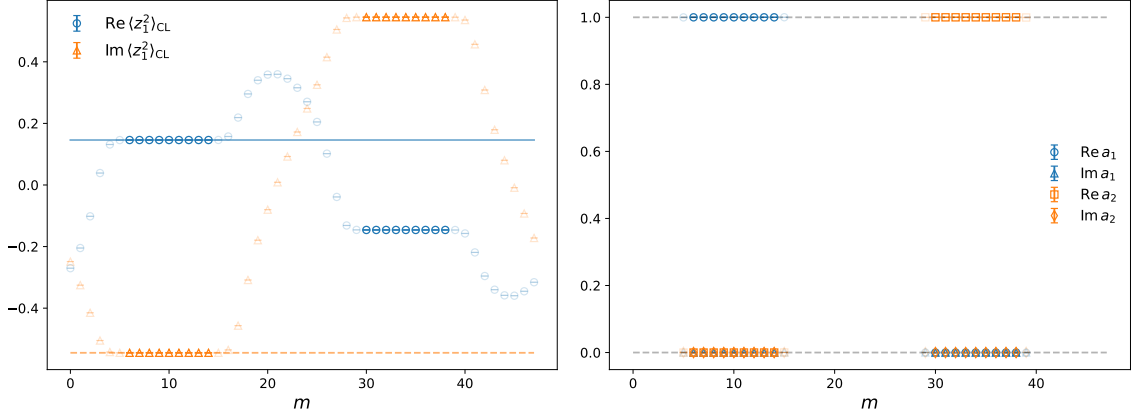
Figure 3: Analogous plots to Fig. 1 for the two-dimensional model (10) with $l = 5$. *Left:* Observable $\langle z_1^2 \rangle$ as a function of m. *Right:* The coefficients a_i determined from (4), see the main text for details.

of two independent integration cycles. The fact that the amount of coupling between the degrees of freedom (drastically) affects the number of independent cycles as well as the special role of the O(2)-symmetric model (10) will be discussed in detail in a forthcoming publication.

Finally, let us discuss the validity of (4) for the two-dimensional case at hand. We use a straightforward generalization of (1) to simulate the Langevin-time evolution of z_1 and z_2, with a scalar kernel $K = K_m$ (see (8)) that acts on z_1 and z_2 in the same way. We follow essentially the same steps as before, but now consider bi-variate monomial observables of the form $\langle z_1^{n_1} z_2^{n_2} \rangle$. As an example analogous to Fig. 1 (left), we show in Fig. 3 (left) the dependence of $\langle z_1^2 \rangle_{\text{CL}}$ on m. There are striking similarities between the two figures as both show plateaus around $m = 10$ and $m = 34$, respectively. The other two plateaus present in Fig. 1, however, are not observed in the two-dimensional model. We thus conjecture that on the first and second plateau we should find $a_i = \delta_{i,1}$ and $a_i = \delta_{i,2}$, respectively, which also implies that both coefficients are entirely real and integer-valued. To substantiate this claim, we show in Fig. 3 (right) the m-dependence of the coefficients a_i, determined from (4) using all observables $\langle z_1^{n_1} z_2^{n_2} \rangle_{\text{CL}}$ for which $n_1 + n_2 \leq 4$ and $n_i \neq 3$. As expected, close to $m = 10$ we indeed find $a_1 = 1$ and $a_2 = 0$ and *vice versa* at $m = 34$. We stress that – as in the one-dimensional case – we always obtain stable fits for the a_i when the boundary terms vanish, as predicted by (4).

The observations discussed here are first evidence that the theorem (4) can indeed be generalized to higher dimensions. If this were the case, it could provide a valuable tool in advancing our knowledge on the influence of kernels on complex Langevin simulations and – in particular – their convergence.

Acknowledgments

References

[1] D. Sexty, *Simulating full QCD at nonzero density using the complex Langevin equation*, *Phys. Lett B.* **729** (2014) 108 [1307.7748].

[2] G. Aarts, E. Seiler, D. Sexty and I.-O. Stamatescu, *Simulating QCD at nonzero baryon density to all orders in the hopping parameter expansion*, *Phys. Rev. D* **90** (2014) 114505 [1408.3770].

[3] Z. Fodor, S.D. Katz, D. Sexty and Török, *Complex Langevin dynamics for dynamical QCD at nonzero chemical potential: A comparison with multiparameter reweighting*, *Phys. Rev. D* **92** (2015) 094516 [1508.05260].

[4] M.W. Hansen and D. Sexty, *Testing dynamical stabilization of Complex Langevin simulations of QCD*, 2405.20709.

[5] K. Boguslavski, P. Hotzy and D.I. Müller, *Stabilizing complex Langevin for real-time gauge theories with an anisotropic kernel*, *JHEP* **2023** (2023) 011 [2212.08602].

[6] D. Alvestad, A. Rothkopf and D. Sexty, *Lattice real-time simulations with learned optimal kernels*, *Phys. Rev. D* **109** (2023) L031502 [2310.08053].

[7] G. Parisi, *On complex probabilities*, *Phys. Lett. B* **131** (1983) 393.

[8] J.R. Klauder, *A Langevin approach to fermion and quantum spin correlation functions*, *J. Phys. A* **16** (1983) L317.

[9] G. Aarts, F.A. James, E. Seiler and I.-O. Stamatescu, *Complex Langevin: etiology and diagnostics of its main problem*, *Eur. Phys. J. C* **71** (2011) 1756 [1101.3270].

[10] M. Scherzer, E. Seiler, D. Sexty and I.-O. Stamatescu, *Complex Langevin and boundary terms*, *Phys. Rev. D* **99** (2019) 014512 [1808.05187].

[11] G. Parisi and Y.-S. Wu, *Perturbation theory without gauge fixing*, *Sci. Sin.* **24** (1981) 483.

[12] M. Scherzer, E. Seiler, D. Sexty and I.-O. Stamatescu, *Controlling complex Langevin simulations of lattice models by boundary term analysis*, *Phys. Rev. D* **101** (2020) 014501 [1910.09427].

[13] L.L. Salcedo and E. Seiler, *Schwinger–Dyson equations and line integrals*, *J. Phys. A* **52** (2019) 035201 [1809.06888].

[14] L.L. Salcedo, *Spurious solutions of the complex Langevin equation*, *Phys. Lett. B* **304** (1993) 125.

[15] H. Okamoto, K. Okano, L. Schülke and S. Tanaka, *The role of a kernel in complex langevin systems*, *Nucl. Phys. B* **324** (1989) 684.

[16] G. Aarts, *Lefschetz thimbles and stochastic quantization: Complex actions in the complex plane*, *Phys. Rev. D* **88** (2013) 094501 [1308.4811].

9